

Lightweight super resolution network for point cloud geometry compression

Wei Zhang^{**}, Dingquan Li^{*}, Ge Li[†], and Wen Gao^{**}

^{*}Peng Cheng Laboratory, Shenzhen, China

^{*}Harbin Institute of Technology, Shenzhen, China

[†]Peking University Shenzhen Graduate School, Shenzhen, China

Abstract

This paper presents an approach for compressing point cloud geometry by leveraging a lightweight super-resolution network. The proposed method involves decomposing a point cloud into a base point cloud and the interpolation patterns for reconstructing the original point cloud. While the base point cloud can be efficiently compressed using any lossless codec, such as Geometry-based Point Cloud Compression, a distinct strategy is employed for handling the interpolation patterns. Rather than directly compressing the interpolation patterns, a lightweight super-resolution network is utilized to learn this information through overfitting. Subsequently, the network parameter is transmitted to assist in point cloud reconstruction at the decoder side. Notably, our approach differentiates itself from lookup table-based methods, allowing us to obtain more accurate interpolation patterns by accessing a broader range of neighboring voxels at an acceptable computational cost. Experiments on MPEG Cat1 (Solid) and Cat2 datasets demonstrate the remarkable compression performance achieved by our method.

Introduction

Point clouds have gained significant popularity due to their remarkable ability to realistically and naturally represent 3D objects. They serve as a versatile media format widely used in numerous immersive multimedia applications, including augmented, virtual, and mixed reality [1]. Point cloud compression (PCC) is a rapidly growing research field focused on creating efficient coding solutions for increasingly large point clouds to meet storage and transmission requirements. Leading standardization bodies, such as the Moving Picture Experts Group (MPEG), the Joint Photographic Experts Group (JPEG), and the Audio Video Coding Standards Workgroup of China (AVS), have dedicated substantial efforts to establish PCC standards [2–6]. Concurrently, there has been a surge of interest in scientific literature, with various researchers working on improved compression methods for point clouds [7–12]. In this context, we focus on point cloud geometry compression, and we review related and representative works in this field below.

Video-based PCC (V-PCC) and Geometry-based PCC (G-PCC) represent two conventional approaches [13]. V-PCC employs 3D-to-2D projections, leveraging well-established video coding techniques for compression. Over time, several enhancements have been introduced to V-PCC, addressing aspects such as rate control, plane projection, reduction of computational complexity, motion prediction, and artifact removal.

The first two authors contribute equally. This work was supported by The Major Key Project of PCL. Corresponding author: Wen Gao.

In contrast, G-PCC operates directly on 3D point clouds, offering the potential for superior compression performance by fully exploiting the inherent data correlations. G-PCC (octree) represents point clouds using an octree structure and encodes the octree using context-based arithmetic coding. G-PCC (trisoup) represents 3D cubes using surfaces composed of triangle strips and encodes the triangles instead of the individual points within these cubes. To enhance the quality of decompressed point clouds in G-PCC, a lookup table-based post-processing super-resolution method has been proposed [10]. Li *et al.* [9] have developed a more accurate lookup table at the encoder side and transmitted it to the decoder to achieve improved super resolution and better rate-distortion optimization. However, it is important to note that the overhead associated with transmitting the lookup table increases exponentially concerning the considered neighboring voxels, even though it leads to reduced distortion. To address this issue, we propose an alternative approach. Instead of transmitting the lookup table, we employ a lightweight super resolution network to approximate it, resulting in a significantly reduced overhead for transmitting the network parameter and a more efficient compression scheme.

There is a growing recognition of the competitiveness of learning-based PCC solutions [7]. Based on the representation form of point clouds, these methods can be broadly classified into three categories: voxel-based, octree-based, and point-based PCC. Voxel-based methods treat the point cloud geometry as a binary signal on a voxel grid and employ 3D (sparse) convolutions [11, 14]. Octree-based methods represent the point cloud geometry using an octree structure and predict the children of the current node based on its neighboring nodes, such as ancestors and siblings [12, 15, 16]. Point-based methods utilize PointNet-like architectures to learn a compact representation for point clouds [17, 18]. It is worth noting that all of these methods train their models on extensive point cloud datasets, and these models are neither lightweight nor tailored to the specific content of the point cloud being compressed.

In contrast, this paper introduces a lightweight super resolution network for content-adaptive point cloud geometry compression. Specifically, we decompose a point cloud into a base point cloud and its interpolation patterns, which are essential for reconstructing the original point cloud. This approach enables us to achieve compression for the original point cloud by effectively compressing both the base point cloud and its interpolation patterns. For the compression of the base point cloud, we employ a pre-existing lossless codec, such as G-PCC or OctAttention [12], to ensure efficient compression. To handle the interpolation patterns, we present an alternative strategy. Instead of directly compressing this information, we opt for overfitting a lightweight super resolution network to learn it. Subsequently, we encode and transmit the content-adaptive network parameter, which facilitates point cloud reconstruction at the decoder side. Our method is validated through experimental verification using the MPEG Cat1 (Solid) and Cat2 datasets. The results of these experiments underscore the effectiveness of our approach, demonstrating significant Bjøntegaard-delta bitrate savings compared to G-PCC (octree) v22 and V-PCC v22.

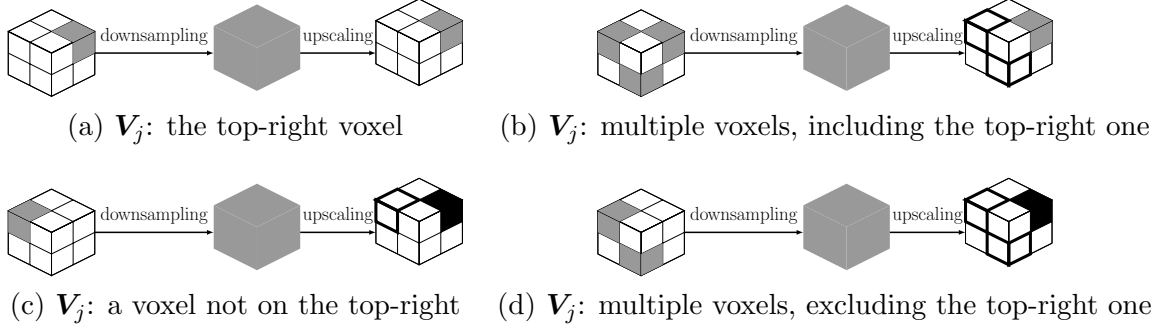


Figure 1: Illustration of possible scenarios during the downsampling and upscaling processes. In each subfigure, the left side depicts the voxelization of a subset \mathbf{V}_j , where the gray-filled cubes represent the presence of points (occupied voxels), and the white-unfilled cubes signify the absence of points (empty voxels). In the middle, following a $2 \times$ downsampling, the point $(x_{d_j}, y_{d_j}, z_{d_j})$ in the downsampled point cloud \mathbf{V}_d is obtained. On the right, upscaling results in the reconstruction of $\hat{\mathbf{V}}_j$, which includes only a single point $(2x_{d_j}, 2y_{d_j}, 2z_{d_j})$. The black-filled cubes represent newly added incorrect points, while the unfilled cubes with black lines indicate the failure to recover the original points.

Background: Downsampling and Upscaling

We represent the original point cloud as $\mathbf{V} = \{(x_i, y_i, z_i)\}_{i=1}^N$ in a voxelized form, where N denotes the number of points. By applying a downsampling operation with a factor of 2 to \mathbf{V} , we obtain a downsampled point cloud, $\mathbf{V}_d = \{(x_{d_j}, y_{d_j}, z_{d_j})\}_{j=1}^M$, denoted as follows:

$$\mathbf{V}_d = \text{unique}([\mathbf{V}/2]). \quad (1)$$

Here, the function `unique` removes any duplicate points, and $[\cdot]$ represents the round-function.

Based on the downsampled point cloud \mathbf{V}_d , the original point cloud \mathbf{V} can be partitioned into M subsets $\{\mathbf{V}_j\}_{j=1}^M$. Each subset, \mathbf{V}_j , encompasses all the points in \mathbf{V} that map to $(x_{d_j}, y_{d_j}, z_{d_j})$ after downsampling, which can be expressed as follows:

$$\mathbf{V} = \bigcup_{j=1}^M \mathbf{V}_j, \quad (2)$$

$$\mathbf{V}_j = \left\{ (x_i, y_i, z_i) \in \mathbf{V} \mid \left\lfloor \frac{x_i}{2} \right\rfloor = x_{d_j}, \left\lfloor \frac{y_i}{2} \right\rfloor = y_{d_j}, \left\lfloor \frac{z_i}{2} \right\rfloor = z_{d_j} \right\}. \quad (3)$$

In accordance with this definition, each subset \mathbf{V}_j comprises a minimum of 1 element and a maximum of 8 elements. Fig. 1 illustrates possible scenarios of downsampling and upscaling processes. Scenario (a) does not induce distortion and allows for the complete recovery of information in \mathbf{V}_j . In all other scenarios, distortions arise due to the inclusion of incorrect points and/or the loss of original points. Only when all $\{\mathbf{V}_j\}_{j=1}^M$ adhere to Scenario (a), encoding \mathbf{V}_d losslessly preserves information about \mathbf{V} , achieving lossless compression of \mathbf{V} .

Proposed Method

There exists a one-to-one or one-to-many mapping between the downsampled point (x_{dj}, y_{dj}, z_{dj}) and its corresponding original points in \mathbf{V}_j for $j = 1, \dots, M$. We refer to this information as *interpolation patterns*, denoted as \mathbf{I}_u . If we encode these interpolation patterns, we can achieve point cloud super resolution using them rather than direct upscaling, which serves to reduce or even remove the aforementioned distortions. In essence, by decomposing the original point cloud into a downsampled point cloud and its corresponding interpolation patterns, the problem of lossy/lossless compression of the original point cloud is transformed into lossless compression of the downsampled point cloud and lossy/lossless compression of the interpolation patterns. This approach resembles the “base layer + enhancement layer” framework commonly used in video coding, such as LCEVC [19]. The downsampled point cloud can be effectively compressed using any lossless codec. The key of our approach hinges on the compression of the interpolation patterns. Directly compressing the interpolation patterns may incur an enormous bitrate cost. Therefore, we propose employing a neural network to predict the interpolation patterns \mathbf{I}_u from the downsampled point cloud \mathbf{V}_d . Subsequently, we encode and transmit the network parameter instead.

Prediction of the Interpolation Pattern

Let $\mathbf{u}_j^{4\delta_x+2\delta_y+\delta_z} = (2x_{dj} - \delta_x, 2y_{dj} - \delta_y, 2z_{dj} - \delta_z)$, where $\delta_x, \delta_y, \delta_z \in \{0, 1\}$. We obtain the interpolation pattern corresponding to the point (x_{dj}, y_{dj}, z_{dj}) in \mathbf{V}_d by determining whether the point \mathbf{u}_j^k belongs to the subset \mathbf{V}_j :

$$I_u(j, k) = \mathbb{I}[\mathbf{u}_j^k \in \mathbf{V}_j], \quad k = 0, \dots, 7, \quad j = 1, \dots, M. \quad (4)$$

Here, $\mathbb{I}[\cdot]$ is the indicator function, taking the value of 1 when the event inside the brackets is true and 0 otherwise. Consequently, the original point cloud can be transformed into the representation of the downsampled point cloud \mathbf{V}_d and its corresponding interpolation patterns \mathbf{I}_u :

$$\mathbf{V} \longrightarrow \{\mathbf{V}_d, \mathbf{I}_u\}. \quad (5)$$

In theory, given that the downsampled point cloud \mathbf{V}_d will be losslessly encoded, we can input all the information of \mathbf{V}_d into a neural network $f(\cdot; \boldsymbol{\theta})$ to predict \mathbf{I}_u :

$$\mathbf{I}_u = f(\mathbf{V}_d; \boldsymbol{\theta}). \quad (6)$$

However, including excessive reference information would increase the complexity of the neural network, which is not conducive to the compression of the neural network. We observe that point clouds exhibit non-local geometric similarities, implying that when the occupancy information of neighboring points in the downsampled point cloud is the same, the interpolation pattern will likely be the same. Let \mathcal{N}_j denote the set of neighbors of the point (x_{dj}, y_{dj}, z_{dj}) in \mathbf{V}_d . The occupancy information can be represented as follows:

$$\mathbf{O}_{\mathcal{N}_j} = \{\mathbb{I}[\mathbf{v} \in \mathbf{V}_d] \mid \mathbf{v} \in \mathcal{N}_j\}, \quad j = 1, \dots, M. \quad (7)$$

Hence, it is feasible to input the occupancy information of the neighbors of (x_{dj}, y_{dj}, z_{dj}) , denoted as $\mathbf{O}_{\mathcal{N}_j}$, into the neural network $f(\cdot; \boldsymbol{\theta})$ to predict its interpolation pattern $\mathbf{I}_u(j)$:

$$\mathbf{I}_u(j) = f(\mathbf{O}_{\mathcal{N}_j}; \boldsymbol{\theta}). \quad (8)$$

Overfitting of Lightweight Super Resolution Network

The design of the network $f(\cdot; \boldsymbol{\theta})$ employs a lightweight multi-layer perceptron (MLP) comprising just one hidden layer. The input dimension of the network corresponds to the number of elements in the neighborhood set \mathcal{N}_j , denoted as $|\mathcal{N}_j|$. The number of neurons in the hidden layer is configured as a small positive integer, for instance, 32, and the output dimension corresponds to the number of elements in the interpolation pattern $\mathbf{I}_u(j)$, which is 8. To introduce non-linear fitting capability, a Sine activation function [20] is employed in the hidden layer, while a Sigmoid activation function is applied to the output layer. The network $f(\cdot; \boldsymbol{\theta})$ contains only a few hundreds or thousands of floating-point numbers, which is significantly smaller compared to networks with millions of parameters.

The prediction of the interpolation pattern can be regarded as eight binary classification problems, and the binary cross-entropy (BCE) loss is used for network overfitting. The BCE loss is formulated as

$$\ell = \frac{1}{M} \sum_{j=1}^M \mathbf{I}_u(j) \log f_j + (1 - \mathbf{I}_u(j)) \log(1 - f_j), \quad (9)$$

where f_j is a simplified representation of $f(\mathbf{O}_{\mathcal{N}_j}; \boldsymbol{\theta})$. Batch-wise training is performed using the Adam optimizer [21] with a learning rate of 0.001, a batch size of 2048, and a total training epochs of 150.

Overall Framework

Finally, we propose an innovative point cloud geometry compression approach based on the overfitted lightweight super resolution network. The overall framework of this approach is visualized in Fig. 2. In the encoding phase, given a point cloud \mathbf{V} and a downsampling factor $q = 2^{-K}$, where $K \in \mathbb{N}_+$, we perform a two-step downsampling to obtain the intermediate and base point clouds as follows:

$$\mathbf{U}^{(K)} = \text{unique}([\mathbf{V}/2^{K-1}]), \quad (10)$$

$$\mathbf{V}^{(K)} = \text{unique}([\mathbf{U}^{(K)}/2]). \quad (11)$$

Subsequently, $\mathbf{U}^{(K)}$ and $\mathbf{V}^{(K)}$ form the pair for overfitting the super resolution network $f(\cdot; \boldsymbol{\theta})$. Then, the network parameter $\boldsymbol{\theta}$ and the base point cloud $\mathbf{V}^{(K)}$ are encoded separately. G-PCC [3] or OctAttention [12] is adopted as the base encoder to losslessly compress $\mathbf{V}^{(K)}$, while the floating-point compression tool fpzip [22] is adopted as the side encoder to compress $\boldsymbol{\theta}$ with a precision of 16 bits. In the decoding phase, the losslessly decoded $\mathbf{V}^{(K)}$ is enhanced with the assistance of the reconstructed super resolution network $f(\cdot; \hat{\boldsymbol{\theta}})$. If the interpolated point cloud has

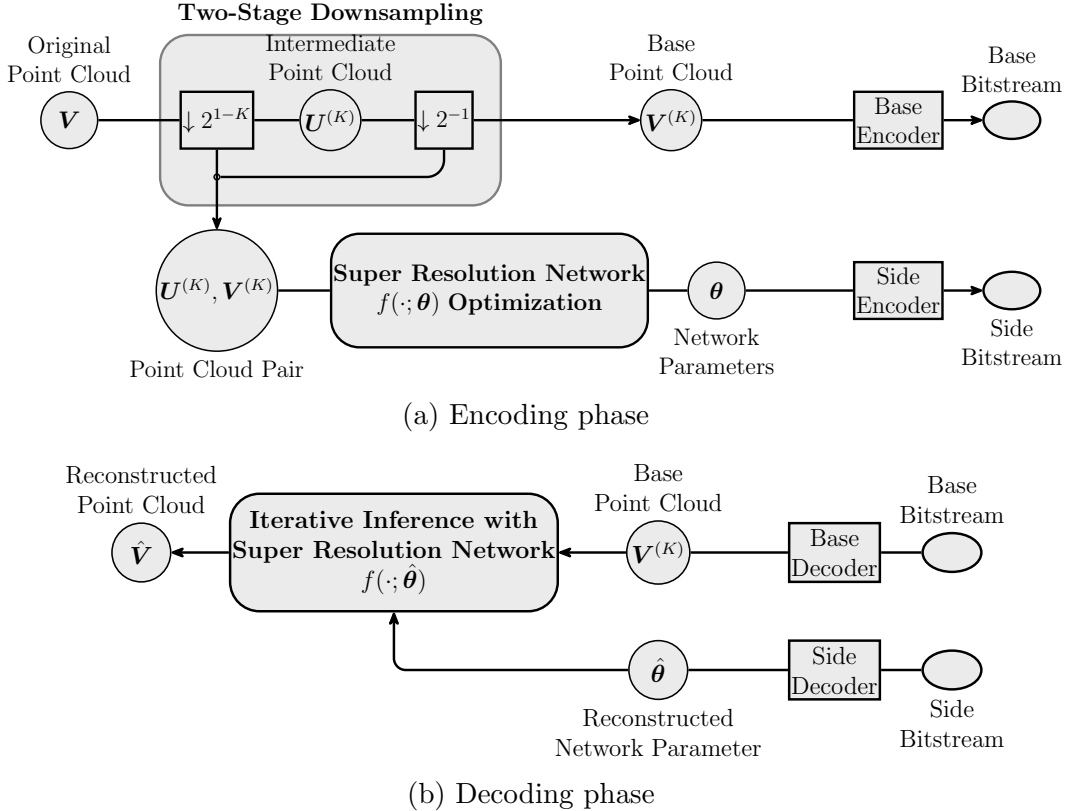


Figure 2: The proposed point cloud geometry compression framework based on the overfitted lightweight super resolution network.

not yet reached the scale of the original point cloud, we apply $f(\cdot; \hat{\theta})$ once more to enhance the reconstruction quality further. Finally, the interpolated point cloud is upscaled to match the scale of \mathbf{V} .

Experiments

The proposed method, named LSRN-PCGC, is evaluated on MPEG Cat1 (Solid) and Cat2 datasets [23, 24]. Six rate points are considered corresponding to $K = 1, 2, 3, 4, 5, 6$, respectively. For Cat1 (Solid), we consider 26 neighbors where the distance along each axis does not exceed $D = 1$ units as the neighborhood set \mathcal{N}_j and set the hidden size of the network to 2^{6-K} correspondingly for balancing the bitrate cost of the base point cloud and the network parameter. For Cat2, we employ a frame sampling rate of 10 to expedite training, while testing on all frames. Since the base bitstream is relatively large, for Cat2, we consider 124 neighbors whose distances to the current point along each axis do not exceed $D = 2$ units, and the hidden size of the network is kept constant at 32. We use point-to-point (D1) distance as the distortion measurement [25] and report the Bjøntegaard-delta bitrate (BDBR) [26] to evaluate rate-distortion performance gains. For those interested in the implementation, it is available at the following URL: <https://github.com/lidq92/LSRN-PCGC>.

Table 1: D1-BDBR savings for LSRN-PCGC against G-PCC v22 [3] and HPSR-PCGC [9]

| Point Cloud | LSRN-PCGC vs. G-PCC | LSRN-PCGC vs. HPSR-PCGC |
|----------------------------------|------------------------|----------------------------|
| basketball_player_vox11.00000200 | -75.0% | -14.0% |
| dancer_vox11.00000001 | -74.7% | -18.3% |
| facade_00064_vox11 | -80.4% | -26.8% |
| longdress_vox10_1300 | -74.9% | -25.7% |
| loot_vox10_1200 | -74.0% | -17.1% |
| queen_0200 | -76.9% | -23.4% |
| redandblack_vox10_1550 | -73.2% | -24.0% |
| soldier_vox10_0690 | -75.8% | -26.9% |
| thaidancer_viewdep_vox12 | -65.4% | -5.5% |
| MPEG Cat1 (Solid) Average | -74.5% | -20.2% |

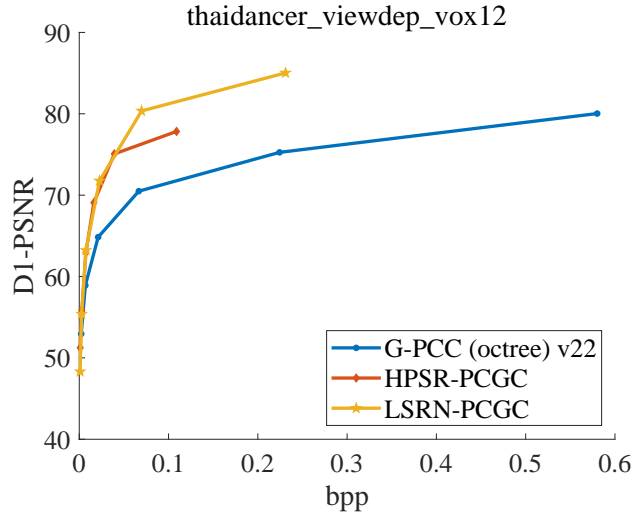


Figure 3: Rate-distortion curves comparison between LSRN-PCGC, HPSR-PCGC, and G-PCC (octree). The horizontal axis represents the rate measurement (bits per point, bpp) for geometry, and the vertical axis represents the distortion measurement (D1-PSNR).

Results on MPEG Cat1 (Solid)

In Table 1, we provide a comparison of LSRN-PCGC with G-PCC (octree) v22 [3] and the lookup table-based method HPSR-PCGC [9]. Compared to G-PCC, LSRN-PCGC exhibits significant D1-BDBR savings, ranging from 65.4% to 80.4%, with an average of 74.5% on the MPEG Cat1 (Solid) dataset. In comparison to HPSR-PCGC [9], LSRN-PCGC achieves an average of 20.2% D1-BDBR savings. This can be attributed to its capability to access more neighbors without incurring an exponential increase in bitrate cost. These results verify the effectiveness of the lightweight super resolution network in improving rate-distortion performance.

In Fig. 3, we closely examine the rate-distortion curves of the point cloud with

Table 2: D1-BDBR savings of LSRN-PCGC against V-PCC v22 [2]

| Point Cloud Sequence | LSRN-PCGC with G-PCC vs. V-PCC | LSRN-PCGC with OctAttention vs. V-PCC |
|--------------------------|--------------------------------------|---|
| loot | -33.8% | -52.2% |
| redandblack | -46.2% | -61.3% |
| soldier | -45.0% | -58.7% |
| queen | -44.6% | -59.0% |
| longdress | -35.3% | -52.7% |
| basketball_player_vox11 | -31.0% | -42.5% |
| dancer_player_vox11 | -35.1% | -46.7% |
| 8iVFB Average | -40.1% | -56.2% |
| MPEG Cat2 Average | -38.7% | -53.3% |

the least D1-BDBR savings (thaidancer_viewdep_vox12). These curves vividly illustrate that both LSRN-PCGC and HPSR-PCGC outperform G-PCC, and the performance gap is substantial. This observation underscores the effectiveness of the super-resolution methods in enhancing the rate-distortion performance. Notably, for the two higher rate points, where the network parameter consumes only a tiny portion of the total bitstream, the lightweight super-resolution network can achieve an improvement of up to 10 dB D1-PSNR over G-PCC while incurring smaller bitrate costs, leading to a better rate-distortion performance than HPSR-PCGC.

Results on MPEG Cat2

In Table 2, we present a comparison between our method and V-PCC v22 [2]. With the aid of the learned lightweight super resolution network, our method utilizing G-PCC (octree) as the base encoder outperforms V-PCC, achieving an average D1-BDBR savings of 38.7% D1-BDBR savings. When using the more advanced base encoder OctAttention [12], our method maintains the same D1-PSNR performance but significantly reduces the bitrate cost for encoding the base point cloud. As a result, it saves more than 50% D1-BDBR compared to V-PCC on the MPEG Cat2 dataset. Additionally, when evaluating the four point cloud sequences (loot, redandblack, soldier, and longdress) from 8iVFB, we observe average D1-BDBR savings of 40.1% and 56.2% for LSRN-PCGC with G-PCC (octree) and OctAttention, respectively. This indicates that LSRN-PCGC, utilizing a lightweight neural network with G-PCC (octree), marginally outperforms the reported performance (39.4%) of PCGCv2 [27] which relies on a large neural network. Furthermore, LSRN-PCGC can significantly outperform PCGCv2 when paired with an advanced base encoder like OctAttention. These results confirm the effectiveness of our method in handling dynamic solid point cloud sequences.

Discussion and Conclusion

We have introduced a content-adaptive approach utilizing a lightweight super-resolution network for lossy point cloud geometry compression. Our experiments on the MPEG Cat1 (Solid) and Cat2 datasets have validated the effectiveness of our proposed method in enhancing rate-distortion performance and its superiority over lookup table-based methods. While this work represents a preliminary stage, it can be extended in several directions. First, incorporating attribute information can enhance the accuracy of predicted interpolation patterns, further improving compression performance. Second, although our method employs a lightweight decoding process, network overfitting increases the encoding time. To address this, we may explore learning a hypernetwork to reduce encoding time. Third, there is potential to investigate joint lossy/lossless compression of point cloud geometry and attributes within this framework, which can be a promising avenue for further research.

References

- [1] Sebastian Schwarz, Marius Preda, Vittorio Baroncini, Madhukar Budagavi, Pablo Cesar, Philip A Chou, Robert A Cohen, Maja Krivokuća, Sébastien Lasserre, Zhu Li, Joan Llach, Khaled Mammou, Rufael Mekuria, Ohji Nakagami, Ernestasia Siahaan, Ali Tabatabai, Alexis M Tourapis, and Vladyslav Zakharchenko, “Emerging MPEG standards for point cloud compression,” *IEEE Journal on Emerging and Selected Topics in Circuits and Systems*, vol. 9, no. 1, pp. 133–148, 2019.
- [2] MPEG 3D Graphics Coding, “V-PCC test model v22,” Output document N00572, ISO/IEC JTC1/SC29/WG7, 142th MPEG meeting, Antalya, April 2023.
- [3] MPEG 3D Graphics Coding, “G-PCC test model v22,” Output document N00571, ISO/IEC JTC1/SC29/WG7, 142th MPEG meeting, Antalya, April 2023.
- [4] MPEG 3D Graphics Coding, “Material for the preparation of the CfP for AI-based graphics coding,” Output document N00684, ISO/IEC JTC1/SC29/WG7, 143th MPEG meeting, Geneva, July 2023.
- [5] André Guarda and Stuart Perry, “Verification model description for JPEG Pleno learning-based point cloud coding v3.0,” Output document N100566, ISO/IEC JTC1/SC29/WG1, 100th JPEG meeting, Covilhã, July 2023.
- [6] AVS PCC, “AVS PCC codec description (in Chinese),” Output document N3603, AVS, 85th AVS meeting, Changsha, June 2023.
- [7] Maurice Quach, Jiahao Pang, Dong Tian, Giuseppe Valenzise, and Frédéric Dufaux, “Survey on deep learning-based point cloud compression,” *Frontiers in Signal Processing*, vol. 2, pp. 846972, 2022.
- [8] Chao Cao, Marius Preda, Vladyslav Zakharchenko, Euee S Jang, and Titus Zaharia, “Compression of sparse and dense dynamic point clouds — methods and standards,” *Proceedings of the IEEE*, vol. 109, no. 9, pp. 1537–1558, 2021.
- [9] Dingquan Li, Kede Ma, Jing Wang, and Ge Li, “Hierarchical prior-based super resolution for point cloud geometry compression,” *Submitted to IEEE Transactions on Image Processing*, 2023.
- [10] Tomás M Borges, Diogo C Garcia, and Ricardo L de Queiroz, “Fractional super-resolution of voxelized point clouds,” *IEEE Transactions on Image Processing*, vol. 31, pp. 1380–1390, 2022.

- [11] Jianqiang Wang, Dandan Ding, Zhu Li, Xiaoxing Feng, Chuntong Cao, and Zhan Ma, “Sparse tensor-based multiscale representation for point cloud geometry compression,” *IEEE Transactions on Pattern Analysis and Machine Intelligence*, vol. 45, no. 7, pp. 9055–9071, 2023.
- [12] Chunyang Fu, Ge Li, Rui Song, Wei Gao, and Shan Liu, “OctAttention: Octree-based large-scale contexts model for point cloud compression,” in *AAAI Conference on Artificial Intelligence*, 2022, pp. 625–633.
- [13] D. Graziosi, O. Nakagami, S. Kuma, A. Zaghetto, T. Suzuki, and A. Tabatabai, “An overview of ongoing point cloud compression standardization activities: Video-based (V-PCC) and geometry-based (G-PCC),” *APSIPA Transactions on Signal and Information Processing*, vol. 9, pp. e13, 2020.
- [14] Dat Thanh Nguyen, Maurice Quach, Giuseppe Valenzise, and Pierre Duhamel, “Learning-based lossless compression of 3D point cloud geometry,” in *IEEE International Conference on Acoustics, Speech and Signal Processing*, 2021, pp. 4220–4224.
- [15] Lila Huang, Shenlong Wang, Kelvin Wong, Jerry Liu, and Raquel Urtasun, “Oct-Squeeze: Octree-structured entropy model for LiDAR compression,” in *IEEE/CVF Conference on Computer Vision and Pattern Recognition*, 2020, pp. 1313–1323.
- [16] Zhili Chen, Zian Qian, Sukai Wang, and Qifeng Chen, “Point cloud compression with sibling context and surface priors,” in *European Conference on Computer Vision*, 2022, pp. 744–759.
- [17] Tianxin Huang and Yong Liu, “3D point cloud geometry compression on deep learning,” in *ACM International Conference on Multimedia*, 2019, pp. 890–898.
- [18] Xuanzheng Wen, Xu Wang, Junhui Hou, Lin Ma, Yu Zhou, and Jianmin Jiang, “Lossy geometry compression of 3D point cloud data via an adaptive octree-guided network,” in *IEEE International Conference on Multimedia and Expo*, 2020, pp. 1–6.
- [19] Stefano Battista, Guido Meardi, Simone Ferrara, Lorenzo Ciccarelli, Florian Maurer, Massimo Conti, and Simone Orcioni, “Overview of the low complexity enhancement video coding (LCEVC) standard,” *IEEE Transactions on Circuits and Systems for Video Technology*, vol. 32, no. 11, pp. 7983–7995, 2022.
- [20] Vincent Sitzmann, Julien Martel, Alexander Bergman, David Lindell, and Gordon Wetzstein, “Implicit neural representations with periodic activation functions,” in *Advances in Neural Information Processing Systems*, 2020, vol. 33, pp. 7462–7473.
- [21] Diederik P Kingma and Jimmy Ba, “Adam: A method for stochastic optimization,” in *International Conference on Learning Representations*, 2015.
- [22] Peter Lindstrom and Martin Isenburg, “Fast and efficient compression of floating-point data,” *IEEE Transactions on Visualization and Computer Graphics*, vol. 12, no. 5, pp. 1245–1250, 2006.
- [23] MPEG 3D Graphics Coding, “Common test conditions for G-PCC,” Output document N00578, ISO/IEC JTC1/SC29/WG7, 142th MPEG meeting, Antalya, April 2023.
- [24] MPEG 3D Graphics Coding, “Common test conditions for V3C and V-PCC,” Output document N00038, ISO/IEC JTC1/SC29/WG7, 132th MPEG meeting, Online, October 2020.
- [25] Rufael Mekuria, Kees Blom, and Pablo Cesar, “Design, implementation, and evaluation of a point cloud codec for tele-immersive video,” *IEEE Transactions on Circuits and Systems for Video Technology*, vol. 27, no. 4, pp. 828–842, 2017.
- [26] Gisle Bjøntegaard, “Calculation of average PSNR differences between RD-curves,” Input document VCEG-M33, Video Coding Experts Group, 13th VCEG Meeting, Austin, Texas, USA, Mar. 2001.
- [27] Jianqiang Wang, Dandan Ding, Zhu Li, and Zhan Ma, “Multiscale point cloud geometry compression,” in *Data Compression Conference*, 2021, pp. 73–82.